

Fluorination of open- and closed-end single-walled carbon nanotubes

S. Kawasaki,^{*a} K. Komatsu,^a F. Okino,^a H. Touhara^a and H. Kataura^b

^a Faculty of Textile Science and Technology, Shinshu University, 3-15-1 Tokida, Ueda 386-8567, Japan. E-mail: skawasa@giptc.shinshu-u.ac.jp

^b Faculty of Science, Tokyo Metropolitan University, 1-1 Minami-osawa, Hachioji, Tokyo 192-0397, Japan

Received 5th January 2004, Accepted 10th February 2004
First published as an Advance Article on the web 18th March 2004

Fluorination was performed for open- and closed-end single-walled carbon nanotubes (SWNTs) by direct reaction of SWNTs with elemental fluorine gas. Structural changes of SWNTs by fluorination were investigated by XRD and Raman measurements. The fluorination mechanism is discussed.

1 Introduction

Fullerenes and carbon nanotubes have attracted much interest since their discovery because of their unique molecular structures.^{1,2} They are also potentially applicable to several fields due to their good electronic and mechanical properties.^{3–6} Furthermore, many researchers are investigating their physical and chemical modification. So far, we have reported on functionalization of fullerenes by fluorination. In our previous papers, it has been shown that fluorination can control the electronic and elastic properties of fullerenes.^{7–9} Fluorination is also considered to be a chemical gateway to functionalization of single-walled carbon nanotube (SWNT) sidewalls.^{10–19} In addition, the physical and chemical properties of fluorinated SWNT itself have been attracting much interest. Since fluorination can be used to modify the electronic properties of SWNTs, it is expected to enable fabrication of metal/semiconductor junctions on a single tube. The fluorinated SWNT sample can then be applied as a cathode material of a lithium battery. Mickelson *et al.*¹¹ reported that sonicating the fluorinated SWNTs in alcoholic solvents produces metastable solutions which are stable from a couple of days to over 1 week, whereas SWNTs are not dissolved in any organic solvents. Therefore, fluorination provides a way to perform solution-phase chemistry of SWNTs. Although there are many interesting reports on fluorinated SWNTs, the detailed structures of fluorinated SWNTs have not been well understood. In the present paper, we discuss the structural properties of fluorinated SWNTs.

2 Experimental

2.1 Preparation of open- and closed-end SWNT samples

SWNT samples used in the present study were prepared by a laser-ablation method. The detailed procedures of synthesis,

purification and tube-end treatment are described elsewhere.²⁰ We have performed Ar gas adsorption measurements at 87 K for open- and closed-end SWNT samples and confirmed that open-end samples adsorb almost twice the quantity of Ar gas compared with closed-end samples. For convenience, open- and closed-end SWNT samples are abbreviated as o-SWNT and c-SWNT, respectively.

2.2 Fluorination of SWNT samples

Fluorinated SWNT samples were synthesized by direct reaction of SWNTs with elemental fluorine gas as follows. Before fluorination, SWNT samples were heated at 473 K under vacuum for several hours in order to eliminate adsorbed water. The dried SWNT samples were fluorinated with 1 atm F₂ gas at 300 K, 473 K and 523 K for 1 month, 5 h and 5 h, respectively. Abbreviated sample names and fluorination conditions are summarized in Tables 1 and 2.

2.3 Characterization of fluorinated SWNT samples

In order to determine the fluorine content of the samples, X-ray photoelectron spectroscopic (XPS) measurements were performed on an Ulvac-phi model 5600 using non-monochromatized Mg K α X-rays at 1253.6 eV. The XPS spectra were observed at pressures below 10⁻⁷ Pa. The charging effect correction was made by vacuum deposition of gold metal on to the samples, and the photoelectron line of Au 4f_{7/2} (84.1 eV) was used for binding energy calibration. The corrections were *ca.* -0.8 eV.

Powder X-ray diffraction (XRD) experiments were undertaken to investigate the change of SWNT bundle structure by fluorination. An X-ray diffractometer (Rigaku RINT-2200) using Cu K α radiation was used for XRD measurements. Pyrolytic graphite was used as a counter monochromator. For

Table 1 Structural properties of fluorinated o-SWNT samples

| Sample | F/C | Fluorination conditions | | XRD simulation parameters | | | |
|-------------|------|-------------------------|----------|---------------------------|--------------------------|--------------------------|---|
| | | Temp./K | Duration | <i>a</i> /nm | <i>r_c</i> /nm | <i>r_F</i> /nm | <i>I_D</i> / <i>I_G</i> |
| o-SWNT | 0.00 | | | 1.74 | 0.71 | | |
| o-SWNT-F300 | 0.28 | 300 | 1 month | 1.90 | 0.71 | 0.83 | 0.82 |
| o-SWNT-F473 | 0.45 | 473 | 5 h | 1.95 | 0.71 | 0.85 | 0.85 |
| o-SWNT-F523 | 0.51 | 523 | 5 h | 1.97 | 0.71 | 0.85 | 0.87 |

Table 2 Structural properties of fluorinated c-SWNT samples

| Sample | F/C | Fluorination conditions | | XRD simulation parameters | | | I_D/I_G |
|-------------|------|-------------------------|----------|---------------------------|-----------|-----------|-----------|
| | | Temp./K | Duration | a /nm | r_C /nm | r_F /nm | |
| c-SWNT | 0.00 | | | 1.74 | 0.71 | | |
| c-SWNT-F300 | 0.23 | 300 | 1 month | 1.95 | 0.71 | 0.83 | 0.91 |
| c-SWNT-F473 | 0.43 | 473 | 5 h | 1.98 | 0.71 | 0.85 | 1.48 |
| c-SWNT-F523 | 0.48 | 523 | 5 h | 2.00 | 0.71 | 0.86 | 1.56 |

the investigation of individual tube structure, Raman spectra were taken at room temperature using a JASCO NRS-2100F with a charge-coupled device multichannel detector. The excitation source was a 514.5 nm Ar laser line. The laser power was tuned at 70 mW.

3 Results and discussion

Fig. 1(a) and (b) show the observed C 1s and F 1s XPS spectra of the fluorinated o-SWNT samples, respectively. The F/C values in Tables 1 and 2 are determined by the ratio of the integrated intensities of the C 1s and F 1s peaks. This method to evaluate fluorine content by XPS spectra has been used for the investigation of fluorofullerenes and its validity has been confirmed by other elemental analyses (*e.g.*, mass spectroscopy and chemical analysis based on the conventional oxygen flask method.)^{8,21,22} The fluorinated SWNT samples have two main C 1s peaks at around 288 and 285 eV, which are attributed to a carbon bound to a single F atom and a bare carbon, respectively. The ratios of the integrated intensities of these two C 1s peaks are roughly equal to the above-mentioned F/C values. The C 1s and F 1s spectra of c-SWNT samples (not shown) have similar features as shown by Fig. 1(a) and (b). The obtained fluorinated SWNT samples, including o-SWNT-F523 which has the highest fluorine content, are all black and the color change from pristine sample by fluorination was not observed by the naked eye. This is contrary to the case of fluorofullerenes where the color varies from black (C_{60}), through yellow ($C_{60}F_{36}$), to white ($C_{60}F_{48}$).

Fig. 2(a) and (b) show the observed XRD patterns of the fluorinated o- and c-SWNT samples, respectively. In both cases, it was found that the diffraction peaks shift toward the lower angle side with increasing fluorine content. It is well known that a simple attempt to index the observed XRD

reflections with a triangular lattice leads to major discrepancies in diffraction peak positions because the small crystalline coherency and the oscillating molecular scattering factor of SWNT modulate the positions and shapes of the diffraction peaks.³ Therefore, full pattern analysis is necessary to determine the triangular lattice constant by simulating the observed XRD pattern. In the present study, simulation has been performed by using 0th order cylindrical Bessel function $J_0(QR)$ for the SWNT form factor, where Q and R denote the scattering vector and the carbon tube radius, respectively. The main parameters in the simulation are the triangular lattice constant a and tube radius R , and the minor parameters are peak broadenings and thermal factors. The calculated profile is very sensitive to both a and R . We determined these two parameters by a trial and error procedure. Fig. 3(a) shows the observed and simulated XRD patterns of a pristine SWNT sample. As shown in Fig. 3(a), the agreement between the observed and simulated patterns is satisfactory. For the simulation of the fluorinated SWNT samples, the attached fluorine atoms are assumed to form a single fluorine tube and a model consisting of two concentric tubes of carbon and fluorine was used to simplify the model. For such a model, the fluorinated SWNT form factor can be expressed by $F_C J_0(QR) + \alpha F_F J_0(QR')$, where R' denotes the radius of the fluorine tube, α corresponding to the F/C value, F_C and F_F are the atomic form factors of carbon and fluorine atoms, respectively. Fig. 3(b) shows that the simulated pattern of the fluorinated SWNT sample also reproduces well the observed pattern. Tables 1 and 2 summarize the simulation parameters determined by the above-mentioned procedures. It should be noted that the determined values have some ambiguities because the diffraction intensity of the fluorinated sample is weak and only a few diffraction lines are observed. Fig. 4 shows the triangular lattice constants

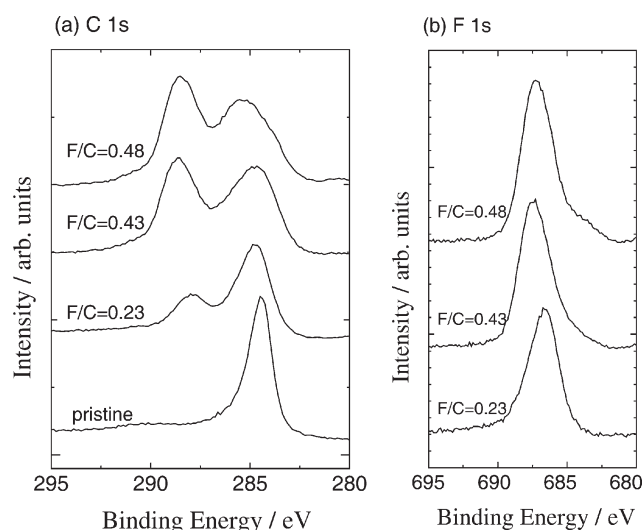


Fig. 1 Observed (a) C 1s and (b) F 1s XPS spectra of fluorinated o-SWNT samples.

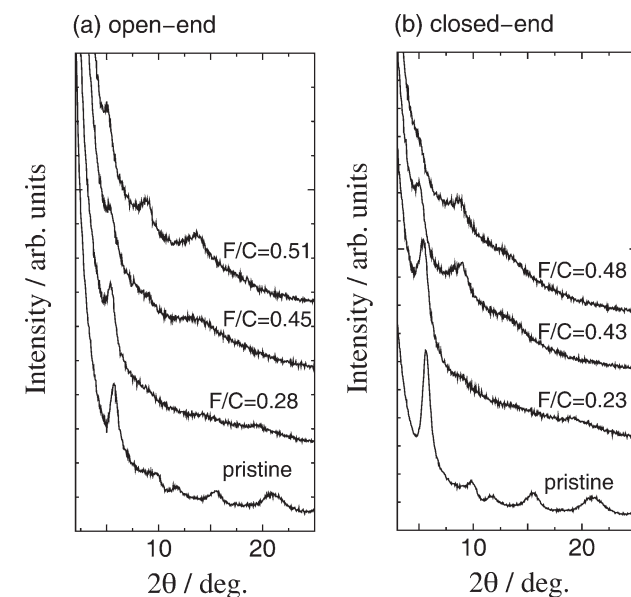


Fig. 2 Observed XRD patterns of (a) o- and (b) c-SWNT samples.

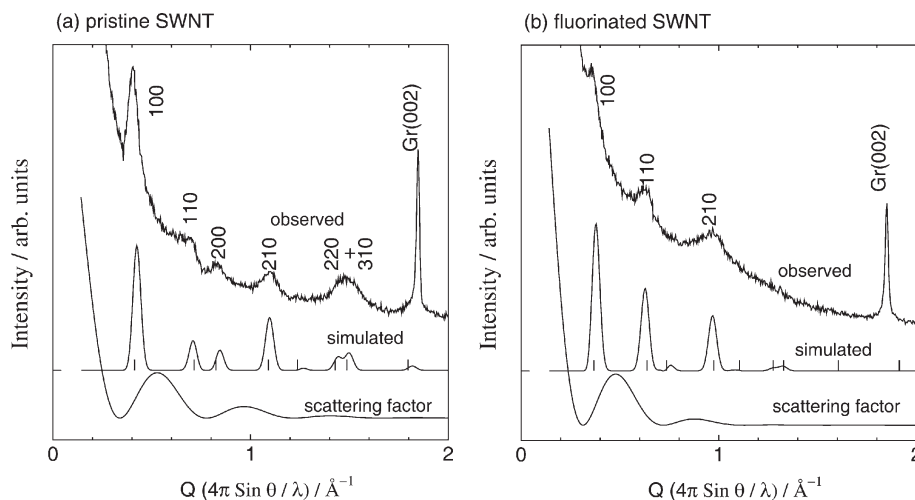


Fig. 3 The comparison between the observed and simulated XRD patterns of (a) pristine and (b) fluorinated SWNT samples. Gr(002) denotes the 002 diffraction line of impurity graphite. Vertical tick marks are the calculated Bragg positions.

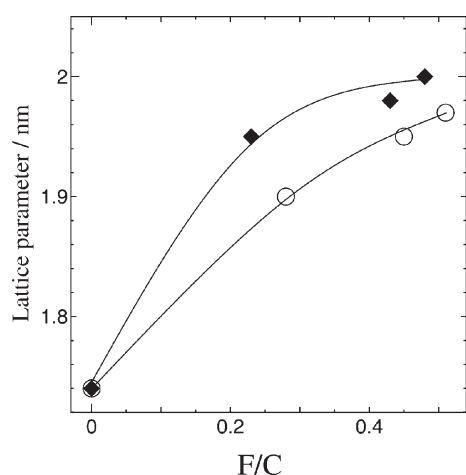


Fig. 4 Lattice parameters of fluorinated SWNT samples as a function of F/C value. Open circles and filled diamonds denote the lattice parameters of fluorinated o- and c-SWNT samples, respectively. The solid lines are the guides to the eye.

of fluorinated o- and c-SWNT as a function of the F/C value. Interestingly, the fluorinated c-SWNT sample has a larger lattice constant than the o-SWNT sample at the same fluorine content.

Fig. 5(a) and (b) show the change in Raman spectrum of o- and c-SWNT samples by fluorination. As shown in Fig. 5(a) and (b), the pristine samples have almost the same Raman spectrum irrespective of the tube-end structure. In the spectra of the pristine samples, since very strong tangential modes (G-band) at $1500\text{--}1600\text{ cm}^{-1}$ and very weak disorder modes (D-band) at about 1340 cm^{-1} , attributed to the defective carbon network, are observed, the purity of the pristine sample is very high. On the other hand, in the spectra of the fluorinated SWNT samples, strong D-bands were clearly observed. This indicates that the coherency of the graphene structure is lowered by fluorine attachment. The ratio of the integrated intensities of D-band and G-band (I_D/I_G) of the fluorinated SWNT samples are summarized in Tables 1 and 2. As shown in Tables 1 and 2, the I_D/I_G values of the fluorinated o-SWNT samples in the range from F/C = 0.28 to F/C = 0.51 are almost the same, whereas the I_D/I_G value increases with fluorine content in the case of the c-SWNT sample. Therefore, in the case of the c-SWNT sample, the degradation of the tube structure continues with increasing fluorine content up to F/C = 0.5, whereas the degree of the degradation of o-SWNT-F300 (F/C = 0.28) is the same as that of o-SWNT-F523 (F/C = 0.51). This interpretation is also supported by the change in radial breathing mode (RBM) (Fig. 6(a) and (b)). As shown in Fig. 6(a), in the case of o-SWNT, sample RBMs are observed even in o-SWNT-F523 which has the highest fluorine content (F/C = 0.51) whereas RBMs are not observed in

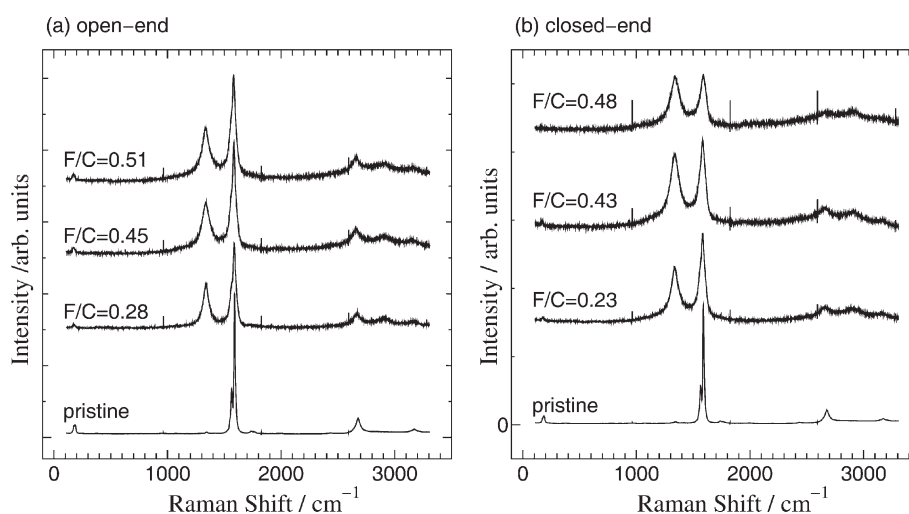


Fig. 5 Observed Raman spectra of fluorinated (a) o- and (b) c-SWNT samples.

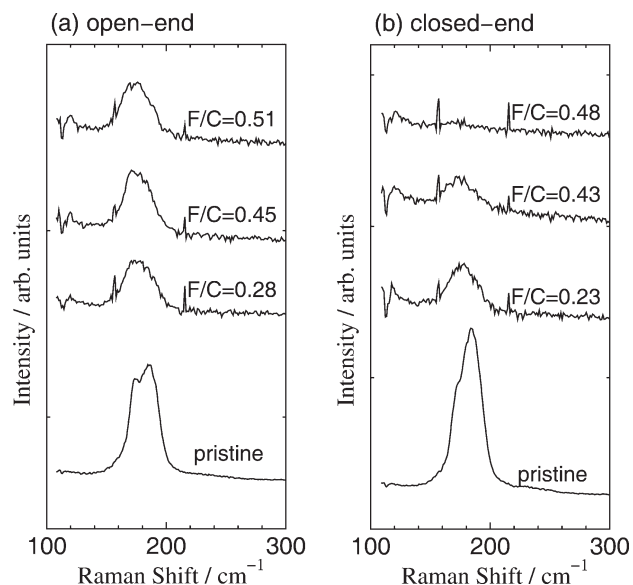


Fig. 6 Observed radial breathing modes of fluorinated (a) o- and (b) c-SWNT samples.

c-SWNT-F523 ($F/C = 0.48$) (Fig. 6(b)). The disappearance of RBMs in c-SWNT-F523 indicates that a large part of the tube is affected by fluorine attachment, while, in the case of o-SWNT samples with the same F/C ratio, some fluorine atoms are attached to the inner and outer sides of the same areas of the wall, leaving a larger area of the wall less affected by fluorination. In both cases of o- and c-SWNT samples, at an early stage of fluorination, the intensity of the higher wave number side of RBM peak decreases and the mean peak position shows downshift. This means that smaller tubes, which are more highly strained and thus have less stable C–C bonds, are selectively fluorinated at an early stage of fluorination.¹⁹

Based on these experimental results, the fluorination mechanism of o- and c-SWNT samples is postulated as follows. The C–C bonds in a certain section of the tube attached with fluorine atoms become unstable and subsequent fluorination may occur selectively at such a section. In the case of o-SWNT sample, since fluorine atoms can access carbon atoms not only from the outside but also from the inside of the tube, fluorine atoms are concentrated in restricted sections, and less-reacted sections of SWNT remain up to $F/C = 0.5$. On the other hand, in the case of c-SWNT sample, since fluorine atoms cannot access the inside of the tube, a larger part of the wall is attacked by the same amount of fluorine atoms compared with o-SWNT samples. It is also understood that the selective fluorination on the outside of c-SWNT tubes results in a larger lattice constant than fluorinated o-SWNT with the same F/C value.

Acknowledgements

The authors are grateful to Mr Narita, Prof. Nagai and Prof. Yamanaka of Osaka University for Raman scattering

experiments. This work was supported in part by a Grant-in-Aid for 21st Century COE Program by the Ministry of Education, Culture, Sports, Science and Technology of Japan, and in part by the Kazuchika Okura Memorial Foundation.

References

- H. W. Kroto, J. R. Heath, S. C. O'Brien, R. F. Curl and R. E. Smalley, *Nature*, 1985, **318**, 162.
- S. Iijima, *Nature*, 1991, **354**, 56.
- A. Thess, R. Lee, P. Nikolaev, H. Dai, P. Petit, J. Robert, C. Xu, Y. H. Lee, S. G. Kim, A. G. Rinzler, D. T. Colbert, G. E. Scuseria, D. Tomanek, J. E. Fischer and R. E. Smalley, *Science*, 1996, **273**, 483.
- V. D. Blank, V. N. Denisov, A. N. Lvlev, B. N. Mavrin, N. R. Serebryanaya, G. A. Dubitsky, S. N. Sulyanov, M. Y. Popov, N. A. Lvova, S. G. Buga and G. N. Kremkova, *Carbon*, 1998, **36**, 1263.
- V. D. Blank, S. G. Buga, N. R. Serebryanaya, G. D. Dubitsky, B. N. Mavrin, M. Y. Popov, R. H. Bargramov, V. M. Prokhorov, S. N. Sulyanov, B. A. Kulnitskiy and Y. V. Tatyani, *Carbon*, 1998, **36**, 665.
- M. Popov, M. Kyotani, R. J. Nemanich and Y. Koga, *Phys. Rev. B*, 2002, **65**, 33408-1.
- S. Kawasaki, F. Okino, H. Touhara and T. Sonoda, *Phys. Rev. B*, 1996, **53**, 16652.
- S. Kawasaki, T. Aketa, F. Okino, H. Touhara, O. V. Boltalina, I. V. Gol'dt, S. I. Troyanov and R. Taylor, *J. Phys. Chem. B*, 1999, **103**, 1223.
- A. Yao, Y. Matsuoka, S. Komiyama, I. Yamada, K. Suito, S. Kawasaki, F. Okino and H. Touhara, *Solid State Sci.*, 2002, **4**, 1443.
- E. T. Mickelson, C. B. Huffman, A. G. Rinzler, R. E. Smalley, R. H. Hauge and J. L. Margrave, *Chem. Phys. Lett.*, 1998, **296**, 188.
- E. T. Mickelson, I. W. Chiang, J. L. Zimmerman, P. J. Boul, J. Lozano, J. Liu, R. E. Smalley, R. H. Hauge and J. L. Margrave, *J. Phys. Chem. B*, 1999, **103**, 4318.
- G. Seifert, T. Kohler and T. Frauenheim, *Appl. Phys. Lett.*, 2000, **77**, 1313.
- H. Peng, Z. Gu, J. Yang, J. L. Zimmerman, P. A. Willis, M. J. Bronikowski, R. E. Smalley, R. H. Hauge and J. L. Margrave, *Nano Lett.*, 2001, **1**, 625.
- K. N. Kudin, H. F. Bettinger and G. E. Scuseria, *Phys. Rev. B*, 2001, **63**, 45413-1.
- H. F. Bettinger, K. N. Kudin and G. E. Scuseria, *J. Am. Chem. Soc.*, 2001, **123**, 12849.
- Z. Gu, H. Peng, R. H. Hauge, R. E. Smalley and J. L. Margrave, *Nano Lett.*, 2002, **2**, 1009.
- W. Zhao, C. Song, B. Zheng, J. Liu and T. Viswanathan, *J. Phys. Chem. B*, 2002, **106**, 293.
- P. R. Marcoux, J. Schreiber, P. Batail, S. Lefrant, J. Renouard, G. Jacob, D. Albertini and J. Mevellec, *Phys. Chem. Chem. Phys.*, 2002, **4**, 2278.
- P. E. Pehrsson, W. Zhao, J. W. Baldwin, C. Song, J. Liu, S. Kooi and B. Zheng, *J. Phys. Chem.*, 2003, **107**, 5690.
- H. Kataura, Y. Maniwa, M. Abe, A. Fujiwara, T. Kodama, K. Kikuchi, H. Imahori, Y. Misaki, S. Suzuki and Y. Achiba, *Appl. Phys. A*, 2002, **74**, 349.
- F. Okino, H. Fujimoto, R. Ishikawa and H. Touhara, *Trans. Mater. Res. Soc. Jpn.*, 1994, **14B**, 1205.
- N. Liu, H. Touhara, F. Okino and S. Kawasaki, *J. Electrochem. Soc.*, 1996, **143**, 2267.